Highly-efficient electrochromic performance of nanostructured TiO_2 films made by doctor blade technique

Nguyen Nang Dinh,[a] Nguyen Minh Quyen, Do Ngoc Chung

University of Engineering and Technology, Vietnam National University, Hanoi 144, Xuan Thuy, Cau Giay, Hanoi,Vietnam.

Marketa Zikova

Czech Technical University in Prague, Zikova 1905/4, 166 36 Prague 6, Czech republic.

Vo-Van Truong

Department of Physics, Concordia University,

1455 de Maisonneuve Blvd W, Montreal (Quebec) Canada H3G 1M8

[a] Electronic mail: dinhnn@vnu.edu.vn (Nguyen Nang Dinh)

Abstract.

Electrochromic TiO_2 anatase thin films on F-doped tin oxide (FTO) substrates were prepared by doctor blade method using a colloidal solution of titanium oxide with particles of 15 nm in size. The films were transparent in the visible range and well colored in a solution of 1M $LiClO_4$ in propylene carbonate. The transmittances of the colored films were found to be strongly dependent on the Li^+ inserted charges. The response time of the electrochromic device coloration was found to be as small as 2 s for a 1 cm^2 sample and the coloration efficiency at a wavelength of 550 nm reached a value as high as 33.7 $cm^2 \times C^{-1}$ for a 600 nm thick nanocrystalline TiO_2 on a FTO-coated glass substrate. Combining the experimental data obtained from in-situ transmittance spectra and in-situ X-ray diffraction analysis with the data from chronoamperometic measurements, it was clearly demonstrated that Li^+ insertion (extraction) into (out of) the TiO_2 anatase films resulted in the formation (disappearance) of the $Li_{0.5}TiO_2$ compound. Potential application of nanocrystalline porous TiO_2 films in large-area electrochromic windows may be considered.

I. INTRODUCTION

Electrochromism is a topic that has attracted a great deal of interest from researchers because of its potential application in various areas (photonics, optics, electronics, architecture, etc). Electrochromic (EC) properties can be found in almost all the transition-metal oxides and their properties have been investigated extensively in the last decades [1]. These oxide films can be coloured anodically (Ir, Ni) or cathodically (W, Mo); however, WO_3 is clearly the preferred material for applications. This is principally due to the fact that WO_3-based electrochromic devices (ECD) have normally a faster response time to a change in voltage and a larger coloration efficiency (CE) as compared to devices based on other electrochromic materials. Recently Granqvist et al. [2] have made a comprehensive review of nanomaterials for benign indoor environments. In this report, the authors show the characteristic data for a 5×5 cm^2 flexible EC foil incorporating WO_3, and NiO modified by the addition of a wide bandgap oxide such as MgO or Al_2O_3, PMMA-based electrolyte, and ITO films. Durability of the EC devices was demonstrated in performing several tens of thousands of coloration/bleaching cycles, and the device optical properties were found to be unchanged for many hours. To improve further the electrochromic properties, Ti-doped WO_3 films were deposited by co-sputtering metallic titanium and tungsten in a Ar/O_2 atmosphere [3]. The optical modulation was found to be around 70% and CE was 66 cm^2/C. Another way to improve electrochromic properties of thin films is to use nanostructured crystalline films. For instance, nanocrystalline WO_3 films were prepared by the organometallic chemical vapour deposition (OMCVD) method using tetra(allyl)tungsten. The size of grains found in these films was estimated by atomic force microscope (AFM) and scanning electron microscope (SEM) to be $20 \div 40$ nm. The coloration of WO_3 deposited on indium-tin- oxides (ITO) substrates (WO_3/ITO) in 2M HCl was less than 1sec and the maximum coloration efficiency at 630 nm was 22 $cm^2\times mC^{-1}$ [4]. However, the HCl electrolyte is not suitable for practical use. A slight improvement was achieved by using gold nanoparticles as

dopants in WO_3. The Au-doped WO_3 films were made by a dip-coating technique [5]. With fabrication of nanostructured WO_3 films Beydaghyan *et al* [6] have shown that porous and thick WO_3 films can produce a high CE. The open structure, fast response and high normal state transmission made them good candidates for use in practical applications. We also have shown that nanocrystalline TiO_2 anatase thin films on ITO prepared by sol-gel dipping method exhibited a good reversible coloration and bleaching process [7]. The lowest transmittance of 10% was obtained at the wavelength of 510 nm for full coloration (65% at the same wavelength in open circuitry). The coloration state was attributed to the formation of the compound $Li_{0.5}TiO_2$ according to the cathodic equation $TiO_2 + 0.5(Li^+ + e^-) \leftrightarrow Li_{0.5}TiO_2$. However the full coloration time was found to be large (i.e. 45 min) and CE was still small (i.e. 15 $cm^2 \times C^{-1}$).

Recently [8], by using the so-called "doctor blade" method, nanoporous TiO_2 anatase films onto F-doped tin oxide (FTO) substrates (nanocrystalline-TiO_2/FTO) or (nc-TiO_2/FTO) were fabricated for dye-sensitized solar cells (DSSC). During the cyclic voltammetry (CV) characterization in $LiClO_4$ + propylene carbonate ($LiClO_4$+PC), it was observed that by applying a cathodic potential, the transmission of nc-TiO_2/FTO changed from being transparent state to a deep blue colour with a response time less than 5 sec. This prompted us to prepare the nanoporous TiO_2 films using the doctor blade technique for the ECD application. Electrochromic properties of the films were characterized by using both *in situ* transmittance spectra and the X-ray diffraction analysis.

II. EXPERIMENTAL

To prepare nanostructured TiO_2 films for ECD, a doctor blade technique was used following the process reported in [8]. However, for ECDs, the nanoporous films should be made with a much smaller thickness, e.g. less than 1 μm. We therefore used two thin adhesive tapes (30 μm in thickness) put parallel and 1 cm apart from each other, creating a slot on the FTO-coated glass slide to contain the colloidal solution. A glass slide overcoated with a 0.2 μm thick FTO film

having a sheet resistance of 15 Ω/□ and a transmittance of 90% was used as a substrate; the useful area that constitutes the sample studied was of 1 cm^2. A colloidal solution of 15 wt % nanoparticles (15 nm in size) of titanium oxide (Nyacol Products) in water was used. For producing thinner films we added more distilled water to get ca. 5 wt % TiO_2 and a few drops of the liquid surfactance were added. Then the diluted solution was filled in the slot on the FTO electrode and spread along the tapes. The samples were left for drying during 15 min before annealing at 450°C in air for 1 hour.

The thickness and surface morphology of the films were measured by field-emission scanning electron microscope (FE-SEM). X-ray diffraction analysis (XRD) was done on a Brucker "Advance-8D" X-ray diffractometer. Electrochemical processes were carried-out by using an AUTOLAB-POTENTIOSTAT-PGS-30 electrochemical unit in a standard three-electrode cell, where TiO_2/FTO served as working electrode (WE), a saturated calomel electrode (SCE) as reference electrode and a platinum grid as counter electrode. 1M $LiClO_4$ + propylene carbonate ($LiClO_4$ + PC) solution was used for electrolyte. All measurements were executed at room temperature.

By using a JASCO "V-570" photospectrometer, *in situ* transmittance spectra of nc-TiO_2 in $LiClO_4$+PC vs. time were recorded on the TiO_2 films of the WE mounted into a modified electrochemical cell which was placed under the pathway of the laser beam and the three cell electrodes were connected to a potentiostat. The same modified electrochemical cell was used for *in situ* XRD analysis to observe structure change during the electrochromic performance, using the above mentioned X-ray diffractometer with X-ray Cu wavelength $\lambda = 0.154$ nm.

III. RESULTS AND DISCUSSION

3.1. Morphology and crystalline structure

The thickness of the films was found to be depending on preparation conditions such as the concentration of solutions and the spread speed. The samples used for further investigation were taken from films chosen with a concentration of 5 wt % TiO_2 in water and a spread speed of 8 mm/s. The bright-field micrographs of the films are shown in Fig. 1a. The thickness of the film was measured from a FE-SEM scanned at a cross section of the film by point-to-point marking technique, as shown in Fig. 1b. The film is well uniform, but some crystallized nanoparticles are a little larger than the initial TiO_2 particles dispersed in water (namely 20 nm in size). The thickness of the films ranges from 500 to 700 nm. In comparison with the nanostructured films prepared by sol-gel method [7] these films are thicker and much more porous. Although the nc-TiO_2 particles are attached to each other tightly, between them there are numerous nanoscale pores which favour the insertion of ions like Li^+ or Na^+ into the films, when a polarized potential is applied on the working electrode (nc-TiO_2/FTO).

The crystalline structure of the films was confirmed by using an accessory for films with a small angle of the X-ray incident beam. For such a thick TiO_2 film, all XRD patterns of the FTO substrate do not appear. Thus the XRD diagram shows all the diffraction peaks corresponding to the titanium oxide. Indeed, in Fig. 2 there are three diffraction peaks which are quite consistent with the peaks for a single crystal of TiO_2 anatase. Those are the most intense peak of the (021) direction corresponding to d = 0.240 nm and two smaller peaks (022) and (220) corresponding to 0.183 nm and 0.174 nm, respectively. The fact that the peak width is rather small shows that the TiO_2 anatase film was crystallized into large grains. To obtain the grain size τ we used the Scherrer formula:

$$\tau = \frac{0.9\lambda}{\beta.\cos\theta} \qquad (1)$$

where λ is wavelength of the X-ray used (λ = 0.154 nm), β the peak width of half height in radians and θ the Bragg angle of the considered diffraction peak [9]. From the XRD patterns the half-height peak width of the (021) direction with $2\theta = 37.415^0$ was found to be β = 0.0053, consequently the size of (021) grain was determined as $\tau \approx 25$ nm. Similarly, the sizes for the (022) and (220) grains were found to be ca. 30 and 20 nm, respectively. This is in good agreement with data obtained by FE-SEM for the average size of particles when the crystalline grains were not identified (see Fig. 1a).

3.2. Electrochemical property

Fig. 3 shows the cyclic voltammetry (CV) curve in $LiClO_4$ + PC of a nc-TiO_2/FTO film, the CV spectra being recorded at the fifth cycle. Such a curve is typical of films prepared in our studies with a thickness of 600 nm. From this figure one can see the symmetrical shape of the CV spectra. In the positive sweep direction (PSD) a peak of the anodic current density corresponding to a value of ca. 0.23 mA was obtained at a potential of –1.10 V/SCE. A slight smaller value (0.19 mA) of the peak in the negative sweep direction (NSD) was obtained at a potential of –0.38 V/SCE. The symmetrical CV proves a good reversibility of the processes of Li^+ ion insertion / extraction from the electrolyte into /out of the working electrode (nc-TiO_2/FTO). The corresponding anodic and cathodic reactions are expressed as follows [10]:

$$TiO_2 + x\,(Li^+ + e^-) \leftrightarrow Li_xTiO_2 \qquad (2)$$

With the help of Raman spectra we confirmed that $0 < x \leq 0.5$ [7].

To study the durability of the porous TiO_2 films, a 2×2 cm^2 WE was measured in 1M $LiClO_4$ + PC for a number of cycles as large as 500 cycles (Fig. 4). From the fifth to tenth cycle, in both the PSD and NSD the current density in absolute value was found to increase; it then slowly decreased. After 500 cycles, the CV curve was maintained unchanged and the current density lowered to a value of 85% of the initial value (at the saturation coloration state, i.e, at the tenth

cycle of the cyclic voltametry). This demonstrates that the Li^+ insertion (extraction) into (out of) the porous TiO_2 films could be easily performed.

For the TiO_2 films deposited by the sol-gel technique, the time to get a saturated state of coloration was as large as 45 min for a sample size of 1 cm^2 [7]. In the present work, the nc-TiO_2/FTO was coloured very rapidly for a sample of the same size. The saturated coloration was reached about 5 sec after a negative potential of –1.20 V/SCE was applied to the WE in the 1M $LiClO_4$ + PC electrolyte. A deep blue colour was observed in the coloration state and a completely transparent bleaching state was obtained after less than 5 sec.

Fig. 5 presents a chronoamperometric plot obtained by setting-up six lapses of 5 sec (see the inset of Fig. 4) for the coloration and bleaching, corresponding to – 1.20 V/SCE and to + 1.20 V/SCE, respectively. To calculate the inserted charge (Q) for the coloration state we use the formula for integrating between the starting and ending time of each lapse of time as follows

$$Q = \int_{t_1}^{t_2} J(t)dt \tag{3}$$

For instance, for the insertion process taking from A to B points, where the integrated area appears as a grey area in Fig. 5, the charge was found to be Q_{in} = 61 mC×cm^{-2}. Whereas for the extraction process taking from C to D points the charge was Q_{ex} = 59 mC×cm^{-2}, that is slightly different from the insertion charge. The fact that the insertion and extraction charges are similar proves that the electrochromic process was a good reversible one - a desired characteristic for the electrochromic performance of the TiO_2-based electrochromic display.

3.3. Electrochromic performance

For a sample with a 600 nm-thick nc-TiO_2 fim on FTO-coated glass, the *in situ* transmission spectra, obtained during coloration at a polarized potential of –1.2 V/SCE are given in Fig. 6. The first spectrum (curve 1) is the transmittance in open circuit. The plots denoted by numbers from 2, 3, 4 and 5 and correspond respectively to coloration times of 0.5, 1, 1.5 and 2sec. The

curve 6 is of the saturated coloration, the completely bleached state occurred also fast, after approximately 2 sec (curve 7). At λ = 550 nm (for the best human-eye sensitivity) the transmittance of the open circuit state is as high as 78%, whereas the transmittance of the saturated coloration state is as low as 10% (see curves 1 and 6 in Fig. 6).

For all the visible range, the complete bleaching of the device occurred much faster than the saturation coloration, as seen in Fig. 7. The bleaching and coloration processes were measured under the application of negatively and positively polarized voltage to the WE, respectively. These processes were clearly associated to the Li^+ insertion (extraction) from the $LiClO_4$+PC electrolyte into (out of) the nc-TiO_2/FTO electrode. Similarly to the results reported previously [2], we attained a transmittance at λ = 550 nm (T_{550}) equal to 73% upon bleaching and to 23% after a coloration period of 40s. The largest optical modulation was observed for red light (T_{700}): the gap between the transmittances of bleaching and coloration states was of 60%. For blue light (T_{400}) the optical modulation at wavelength 400 nm was much smaller, i.e. about 22%. This would result from the strong absorption by both FTO and TiO_2 at shorter wavelengths.

From the above mentioned results, it is seen that the efficient coloration can be attributed to the high porosity of the nc-TiO_2 film. To evaluate the electrochromic coloration efficiency (η) we used a well-known expression relating the efficiency with the optical density, consequently the transmittances of coloration (T_c) and bleaching states (T_b), and the insertion charge (Q) are as follows [11]:

$$\eta = \frac{\Delta OD}{Q} = \frac{1}{Q}\ln\left(\frac{T_b}{T_c}\right), \tag{4}$$

The λ-η plot for the electrochromic performance is shown in Fig. 8. At a wavelength of 550 nm, Q = 0.61 $mC\times cm^{-2}$, T_b = 78% and T_c = 10%, the coloration efficiency was determined to be 33.7 $cm^2\times C^{-1}$. The larger is the wavelength, the higher is the coloration efficiency. In the visible range of wavelengths all the values of η found are comparable to those for WO_3 films [12] and

much higher than those for TiO_2 films [7] prepared by sol-gel techniques and titanium-lanthanide oxides deposited by magnetron sputtering and coloured in a $LiClO_4$ + PC solution [13].

To elucidate the structure change during the electrochromic performance, we carried out *in situ* XRD analysis of the WE which was filled in the $LiClO_4$ + PC solution and connected to a dc-voltage of –1.2 V. Fig. 9 presents *in situ* X-ray patterns of a TiO_2/FTO sample for three states: as-prepared (*ex-situ* pattern, A), after full intercalation which corresponds to the saturation state of coloration (*in-situ* pattern, B) and after complete bleaching (*in-situ* pattern C). Due to the hindrance of the electrolyte in the ECD cell used for the *in situ* XRD set-up, only the largest peak at $2\theta = 37.41^o$ could be revealed However it was seen that this peak is consistent with the (021) plane having the space distance $d_{021} = 0.240$ nm for TiO_2 anatase.

By applying a cathodic potential (i.e. –1.20 V/SCE) to FTO, the colour of WE became deep-blue, and the XRD diagram showed that the observed peak shifts to a large 2θ (ca. 37.90^o). This peak, as known from the database of crystalline structure files, characterizes the (112) plane with $d_{112} = 0.237$ nm of $Li_{0.5}TiO_2$ anatase. With the switching of the polarization of the WE to a positive potential, namely + 1.20 V/SCE, the WE returned to its original transmission state and the XRD peak of the coloured state disappeared while the peak of TiO_2 anatase was restored (*in-situ* pattern, C). We recorded the *in situ* XRD diagrams of the WE in coloration and bleaching states for 20 times, and obtained always the patterns shown in Fig. 9. Thus, the peak with d = 0.237 nm which is characteristic of the coloration state of the WE can be attributed to the structure of $Li_{0.5}TiO_2$ in case of the lithium intercalation. In comparison with the suggestion of this compound in our previous work [7] this result demonstrates more clearly that the structure of the WE changed from the nanocrystalline TiO_2 anatase into the nanocrystalline $Li_{0.5}TiO_2$.

Hereby, this also confirms the validity of equation (2), with x = 0.5. Experiments were also carried out for samples prepared in similar conditions and the results were found to be similar.

IV. CONCLUSION

Nanostructured porous TiO_2 anatase films with a grain size of 20 nm were deposited on transparent conducting FTO electrodes by a doctor-blade method using a colloidal TiO_2 solution (Nyacol Products). Electrochromic performance of TiO_2/FTO was carried out in 1M $LiClO_4$ + propylene carbonate and a good reversible coloration and bleaching process was obtained. The response time of the ECD coloration was found to be as small as 2 s and the coloration efficiency could be as high as 33.7 $cm^2 \times C^{-1}$. *In situ* transmittance spectra and XRD analysis of the TiO_2/FTO working electrode demonstrated the insertion/extraction of Li^+ ions into anatase TiO_2. Simultaneous use of chronoamperometry and XRD allowed the determination of the compound of the saturated coloration state of WE to be $Li_{0.5}TiO_2$. The results showed that nanostructured porous TiO_2 films can be comparable in property to WO_3 films. Since a large-area TiO_2 can be prepared by the simple doctor blade method, nc-TiO_2 electrode constitutes a good candidate for ECD applications, taking advantage of its excellent properties in terms of chemical stability.

Acknowledgments

This work was supported by the Vietnam National Foundation for Science and Technology Development (NAFOSTED) in the period 2010 – 2011 (Project Code: 103.02.88.09).

References

[1] C. G. Granqvist, Handbook of inorganic electrochromic materials, Elsevier, Amsterdam, 1995.

[2] C. G. Granqvist, A. Azens, P. Heszler, L. B. Kish, L. Österlund, Nanomaterials for benign indoor environments: Electrochromics for "smart windows", sensors for airquality, and photo-catalysts for aircleaning, Sol. Energy Mater. Sol. Cells 91 (2007) 355 – 365.

[3] A. Karuppasamy and A. Subrahmanyam, Studies on electrochromic smart windows based on titanium doped WO_3 thin films , Thin Solid Films 516 (2007) 175 –178.

[4] L. Meda, R. C. Breitkopf, T. E. Haas and R. U. Kirss, Investigation of electrochromic properties of nanocrystalline tungsten oxide thin film, Thin Solid Films 402 (2002)126 – 130.

[5] N. Naseri, R. Azimirad, O. Akhavan and A.Z. Moshfegh, Improved electrochromical properties of sol–gel WO_3 thin films by doping gold nanocrystals, Thin Solid Films 518 (2010) 2250 – 2257.

[6] G. Beydaghyan, G. Bader, P.V. Ashrit, Electrochromic and morphological investigation of dry-lithiated nanostructured tungsten trioxide thin films, Thin Solid Films 516 (2008) 1646 – 1650.

[7] N. N. Dinh, N. Th. T. Oanh, P. D. Long, M. C. Bernard, A. Hugot-Le Goff, Electrochromic properties of TiO_2 anatase thin films prepared by dipping sol-gel method, Thin Solid Films 423 (2003) 70 – 76.

[8] N. N. Dinh, N. M. Quyen, L. H. Chi, T. T. C. Thuy, T. Q. Trung, Characterization of solar cells using nano titanium oxide and nanocomposite materials, AIP Conf. Proc. 1169 (2009) 25 – 31.

[9] B. D. Cullity, Elements of X-Ray diffraction, Addison-Wesley Publishing Company, Inc., Reading, MA, 1978.

[10] G. Campet, J. Portier, S. J. Wen, B. Morel, M. Bourrel, J. M. Chabagno, Electrochromism and electrochromic windows, Active and Passive Elec.Comp., 14 (1992) 225 – 231.

[11] P. M. S. Monk, R. J. Mortimer, D. R. Rosseinsky, Electrochromism: Fundamentals and applications, VCH, Weinheim - New York - Basel - Cambridge - Tokyo, 1995.

[12] P. Delichere, P. Falaras, A. Hugot-Le Goff, WO_3 anodic films in organic medium for electrochromic display devices, Solar Energy Materials 19 (1989) 323 – 333.

[13] L. Kullman, A. Azens, C. Granqvist, Decreased electrochromism in Li-intercalated Ti oxide films containing La, Ce, and Pr, J. Appl. Phys. 81 (1997) 8002-1 ÷ 8002-9.

Captions for figures

Fig. 1. FE-SEM bright-field micrograph of a doctor-blade deposited TiO_2 film: surface view (a) and cross-section (b). The concentration of the colloidal solution was 5 wt.% TiO_2 in water, and the spread speed was 8 mm/s. The thickness d of the film was about 600 nm.

Fig. 2. XRD patterns of a nanocrystalline porous TiO_2 films made by a doctor blade technique after being annealed at 450°C in air for 1 hour. The thickness d of the film was about 600 nm.

Fig. 3. Cyclic voltammetry of TiO_2/FTO in 1M $LiClO_4$+PC; the scanning rate is of 50 mV/s.

Fig. 4. Cyclic voltammetry of TiO_2/FTO in 1M $LiClO_4$+PC from 5-th to 500-th cycle with a scanning rate of 150 mV/s; The area of the WE is $2\times2cm^2$.

Fig. 5. Insertion and extraction of Li^+ ions into/out of the TiO_2 anatase film. The inserted charge of the saturated coloration state and the completely bleaching state (marked area), respectively are Q_{in} = 61 $mC\times cm^{-2}$ and Q_{ex} = 59 $mC\times cm^{-2}$. Insertion process from A to B and extraction process from C to D.

Fig. 6. In situ transmission spectra of the TiO_2/FTO colored in 1M $LiClO_4$ + PC at –1.20 V/SCE versus time. The 1st curve is the transmittance spectra in open circuit; 2, 3, 4 and 5 - the spectra corresponding to respective coloration times of 0.5, 1, 1.5 and 2sec; 6 – saturated coloration state; 7 – completely bleached state.

Fig. 7. Time-dependence transmittance of the nc-TiO_2/FTO during electrochromic performance for three different wavelengths: 400, 550 and 700 nm.

Fig. 8. The wavelength dependence of the ECD efficiency of the nc-TiO_2/FTO electrode colored in 1M $LiClO_4$ + PC electrolyte and under application of –1.20 V/SCE.

Fig. 9. In-situ XRD patterns of a nc-TiO_2/FTO films in 1M $LiClO_4$ + PC. 'A' denotes *ex situ*, 'B' - *in situ* colored at –1.2 V/SCE and 'C' - *in situ* bleached at +1.20 V/SCE.

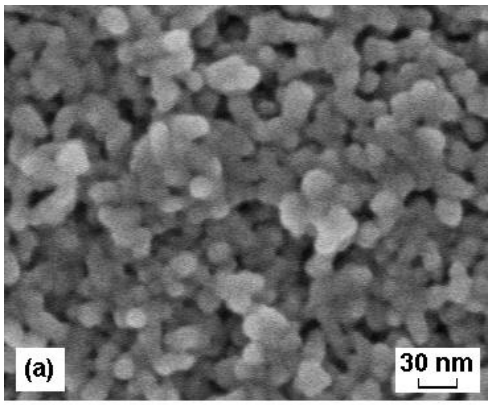

Fig. 1a

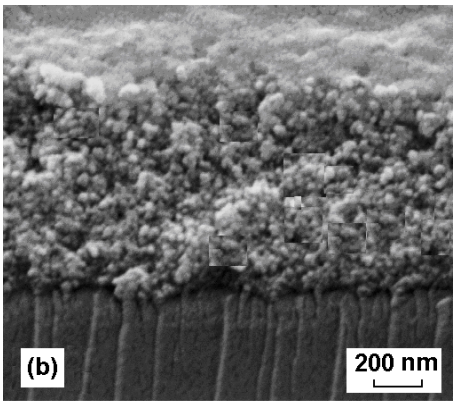

Fig. 1b

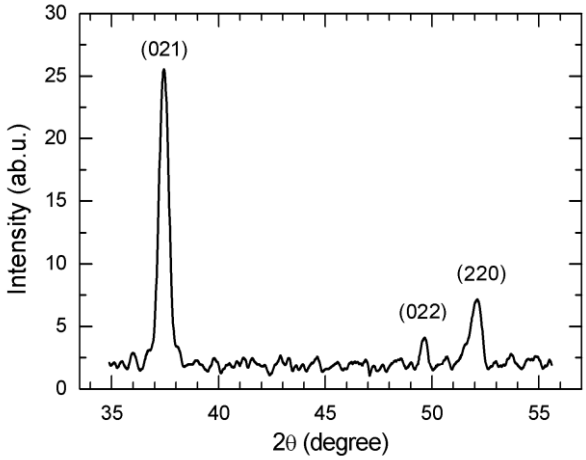

Fig. 2

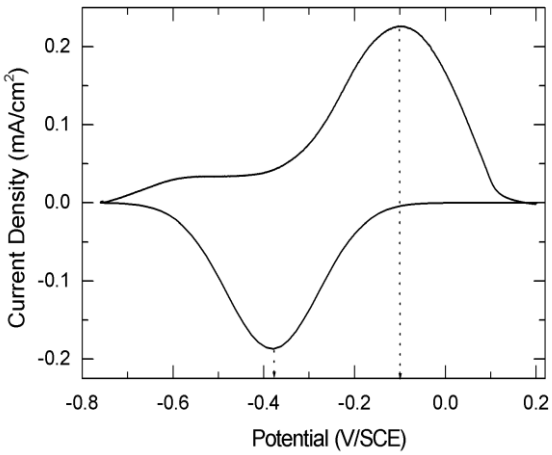

Fig. 3

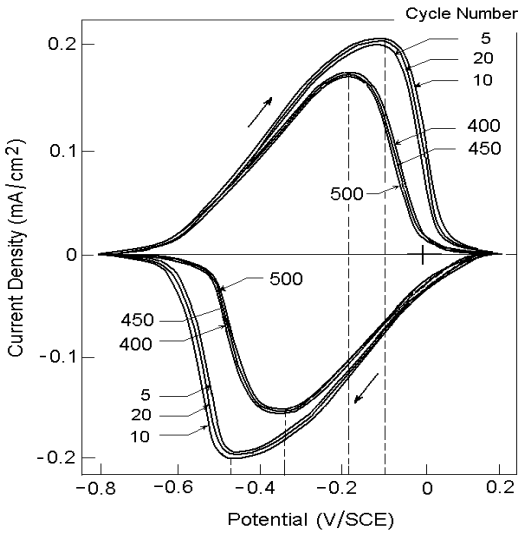

Fig. 4

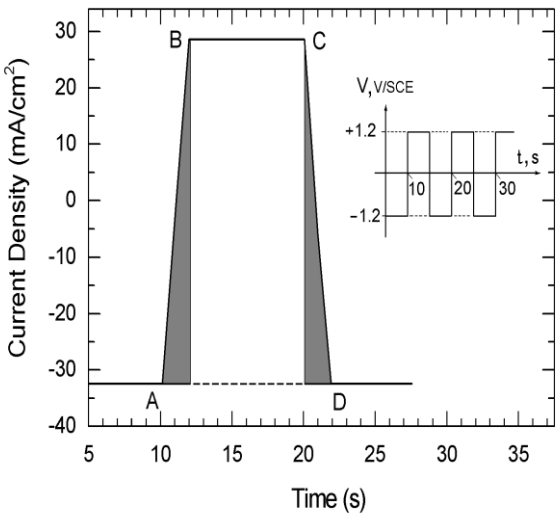

Fig. 5

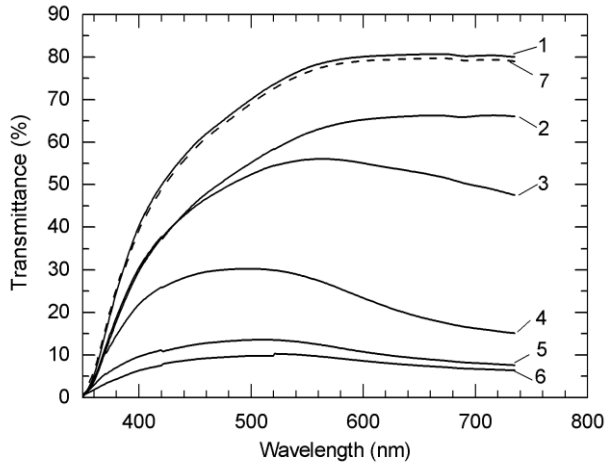

Fig. 6

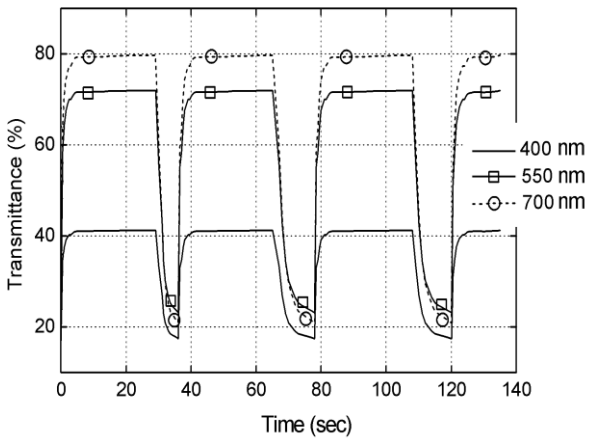

Fig. 7

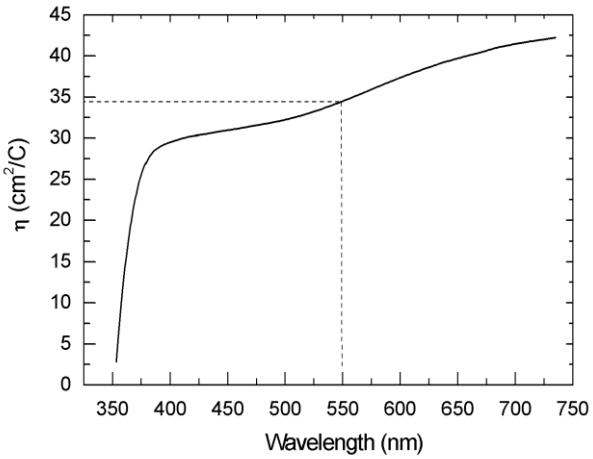

Fig. 8

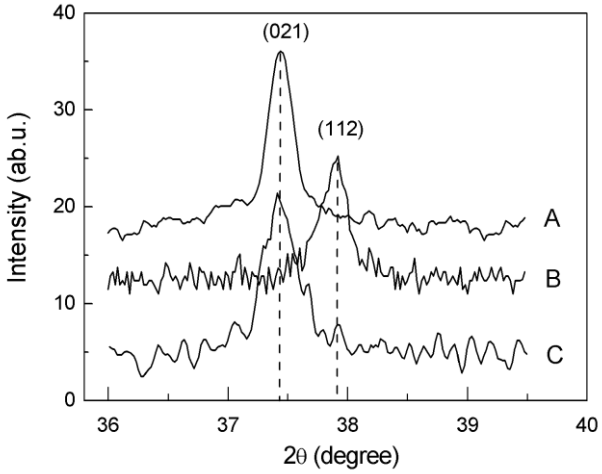

Fig. 9